International Journal of Pharmaceutics 489 (2015) 139–147

Contents lists available at ScienceDirect

International Journal of Pharmaceutics

journal homepage: www.elsevier.com/locate/ijpharm

Evaluation of a combined drug-delivery system for proteins assembled with polymeric nanoparticles and porous microspheres; characterization and protein integrity studies

Sergio Alcalá-Alcalá [a], Claudia G. Benítez-Cardoza [b], Enrique J. Lima-Muñoz [c], Elizabeth Piñón-Segundo [a], David Quintanar-Guerrero [a,*]

[a] Laboratorio de Investigación y Posgrado en Tecnología Farmacéutica, Facultad de Estudios Superiores Cuautitlán, Universidad Nacional Autónoma de México, Avenida 1° de Mayo s/n, Campo 1, Cuautitlán Izcalli, Estado de México CP 54743, Mexico
[b] Laboratorio de Investigación Bioquímica, Sección de Estudios de Posgrado e Investigación, ENMyH-Instituto Politécnico Nacional, Guillermo Massieu Helguera No. 239, La Escalera Ticomán, 07320 D.F., Mexico
[c] Instituto de Investigaciones en Materiales, Universidad Nacional Autónoma de México, Circuito exterior s/n, Cd. Universitaria, Del. Coyoacán, CP 04510 D.F., Mexico

ARTICLE INFO

Article history:
Received 4 December 2014
Received in revised form 4 April 2015
Accepted 27 April 2015
Available online 29 April 2015

Chemical compounds studied in this article:
Poly(D,L-lactide-*co*-glycolide) acid (PubChem CID: 23111554)
2-Chloro-4-nitrophenyl-α-D-maltotrioside (PubChem CID: 9939545)

Keywords:
Adsorption/infiltration
Polymeric nanoparticles
Porous microspheres
Protein delivery
Protein formulation

ABSTRACT

This work presents an evaluation of the adsorption/infiltration process in relation to the loading of a model protein, α-amylase, into an assembled biodegradable polymeric system, free of organic solvents and made up of poly(D,L-lactide-*co*-glycolide) acid (PLGA). Systems were assembled in a friendly aqueous medium by adsorbing and infiltrating polymeric nanoparticles into porous microspheres. These assembled systems are able to load therapeutic amounts of the drug through adsorption of the protein onto the large surface area characteristic of polymeric nanoparticles. The subsequent infiltration of nanoparticles adsorbed with the protein into porous microspheres enabled the controlled release of the protein as a function of the amount of infiltrated nanoparticles, since the surface area available on the porous structure is saturated at different levels, thus modifying the protein release rate. Findings were confirmed by both the BET technique (N_2 isotherms) and *in vitro* release studies. During the adsorption process, the pH of the medium plays an important role by creating an environment that favors adsorption between the surfaces of the micro- and nano-structures and the protein. Finally, assays of α-amylase activity using 2-chloro-4-nitrophenyl-α-D-maltotrioside (CNP-G3) as the substrate and the circular dichroism technique confirmed that when this new approach was used no conformational changes were observed in the protein after release.

1. Introduction

Protein formulation has constituted a significant challenge for the pharmaceutical scientists because the therapeutic activity of these drugs is closely-related to their conformational structure and integrity, and because their physical and chemical instability must be dealt with. Recent advances in biotechnological techniques like fermentation and cloning have made it possible to produce large quantities of biologics (*i.e.*, biotherapeutic proteins) for pharmaceutical applications whose benefits present an opportunity to improve current treatments for disorders such as cancer, genetic and enzymatic deficiencies, autoimmune diseases and infections like HIV (Frokjaer and Otzen, 2005). More than 324 biomacromolecules – mostly proteins – are currently undergoing clinical trials. A general trend is to use drugs produced by recombinant DNA techniques because it is expected that biologics will be less toxic and more predictable regarding their behavior *in vivo* (Pavlou and Reichert, 2010). However, factors such as pH, temperature, high shear forces, interfaces, storage, handling, formulation and administration of such proteins can create undesirable conditions that lead to physical and chemical instability in the form of denaturation, deamidation, aggregation, oxidation, peptide bond hydrolysis, thiol–disulfide exchange, crosslinking, intramolecular conformational scrambling and precipitation processes, all of which can alter their activity (Fu et al., 2000; Krishnamurthy and Manning, 2002; Manning et al., 2010). Thus, the success in formulating proteins requires knowledge and understanding of

* Corresponding author. Tel.: +52 55 56232065; fax: +52 55 58938675.
E-mail addresses: quintana@servidor.unam.mx, sekyaa@gmail.com (D. Quintanar-Guerrero).

http://dx.doi.org/10.1016/j.ijpharm.2015.04.074
0378-5173/

their physical, chemical and biological properties, as well as the use of adequate materials and carriers (Manning et al., 2010).

To facilitate the administration of biologics and to maintain protein integrity during formulation and storage, different drug delivery systems have been proposed. Polymeric and lipid-based nanoparticles (*e.g.,* liposomes), nanocapsules, hydrogels, injectable implants, microemulsions and microspheres are common examples of systems developed to improve protein delivery. Most of these systems are based on entrapment and microencapsulation principles, whose stages basically include emulsification processes and posterior solvent evaporation. Unfortunately, these common manufacturing methods generate a microenvironment that can compromise the protein integrity during drug-loading, microcarrier formation and drying because molecules are exposed to organic solvents, aqueous/organic interfaces, elevated temperatures, vigorous agitation, hydrophobic surfaces and detergents (Van der Weert et al., 2000). Hence, this physicochemical stress affects proteins during the entire life of the drug-delivery system; including formulation, storage and protein release *in vivo* (Dai et al., 2005; Degim and Çelebi, 2007; Sun et al., 2009; Tan et al., 2010; Van der Weert et al., 2000).

Our understanding of protein instability has improved greatly since 1989 and several alternatives, such as stabilization by ligand-binding to the native state (surfactants, polymers, cyclodextrins, metal ions, anion binding, *etc.*), colloidal and interfacial stability, drying, chemical modifications, site-directed mutagenesis and the development of novel drug delivery systems, have been described to protect the integrity of proteins during their life-cycle (Fu et al., 2000; Manning et al., 2010; Wang, 1999). Because research into protein pharmaceutical technology has focused on proposing strategies that will prevent protein damage during formulation, various experiments have been conducted to better understand the critical steps involved in the obtaining of protein drug-delivery systems, instability, and degradation mechanisms (Fu et al., 2000). Polymeric nanoparticles and injectable parenteral depots loaded with peptides and proteins and designed with biodegradable materials like PLGA (polylactide-*co*-glycolide acid) are important in this field, because the protein drug-delivery systems approved by the FDA are based on polymeric microspheres, some of which are already available in the pharmaceutical market (Dai et al., 2005; Degim and Çelebi, 2007; Putney, 1998; Spada et al., 2011). Other approaches, such as incorporating of protein–biopolymers complexes which are then mixed with porous microspheres to obtain self-healing PLGA microspheres, have been proposed to enhance protein loading efficiency and prevent drug instability during encapsulation and release by protein immobilization. The biopolymers used are members of the glycosaminoglycan (GAG) family, or they have similar structural moieties (*e.g.*, dextran sulfate and chitosan) (Shah and Schwendeman, 2014).

On the other hand, adsorption of hydrophilic drugs is a strategy that has been used to avoid high-energy processes in drug entrapment. This approach has been applied successfully to adsorb biomacromolecules onto nanoparticle surfaces (Vrignaud et al., 2011). Many papers have discussed the use of PLGA to adsorb proteins onto micro- and nano-particles in order to avoid the risk of protein degradation caused by the interaction with organic solvents, interfaces, homogenization and drying (Kim et al., 2006a; Sun et al., 2009). The option of using adsorption as an alternative to load drugs takes into account the interaction between the surface of polymeric structures and proteins by establishing and controlling certain variables such as pH, temperature, protein and polymer properties (*e.g.*, isoelectric point, pKa, end functional group, etc.) in an aqueous medium. Recently, the use of porous microspheres with a large pore surface area and interconnecting pores has drawn attention for loading therapeutic drugs (including peptides and proteins) by adsorption in an immersion medium (Kilpeläinen et al., 2011; Rodríguez-Cruz et al., 2009; Sun et al., 2009). The adsorption process and the large surface area of porous microspheres and nanoparticles form the basis of the strategy proposed in earlier research (Alcalá-Alcalá et al., 2013), in which a peptide was formulated using the adsorption/infiltration process. This technique produced assembled systems that load drugs which are sensitive to physicochemical stress with high adsorption efficiencies and a controlled release that are dependent on the continuity of a nanoparticle film that forms on the microsphere surface. The aim of this work was to formulate a globular molecule, a protein (enzyme α-amylase), using the adsorption/infiltration process with biodegradable, PLGA micro- and nano-particles in order to obtain an injectable assembled system with the capacity to release proteins during a week or more. Additionally, the assembled system was characterized and the integrity of the protein after release was evaluated in order to demonstrate the efficacy of this novel protein drug-delivery system.

2. Materials and methods

2.1. Materials

Poly(D,L-lactide-*co*-glycolide) acid (PLGA 50:50, DLG 4A, molecular weight 38,000), was obtained from Lakeshore Biomaterials (Birmingham, AL, USA). α-Amylase (from *Aspergillus oryzae*, 10065-50 G), poly(vinyl alcohol) (PVAL: Mowiol® 4–88, molecular weight 58,000), the Bicinchoninic acid kit for protein determination (BCA1) and 2-chloro-4-nitrophenyl-α-D-maltotrioside (93834 CNP-G3) were purchased from Sigma–Aldrich (St. Louis, MO, USA). Methylene chloride, ethyl acetate, acetonitrile, sodium chloride, calcium chloride, potassium thiocyanate and mannitol were provided by J.T. Baker® Chemicals (Avantor Performance Materials, Center Valley, PA, USA). Ammonium carbonate, monobasic potassium phosphate, sodium citrate, citric acid, acetic acid, sodium acetate and sodium hydroxide were all supplied by Productos Quimicos Monterrey, SA (Monterrey, NL, Mexico). Distilled water was obtained from a RiOs™ distiller (EMD Millipore, Billerica, MA, USA).

2.2. Preparation of the components of the assembled systems

The protein drug-delivery systems were assembled using polymeric nanoparticles and porous polymeric microspheres of PLGA, following well-known and reproducible methods.

2.2.1. PLGA nanoparticles

The emulsification-solvent diffusion method was used to manufacture polymeric nanoparticles (Quintanar-Guerrero et al., 1996). Two phases were prepared after saturation between distilled water (phase W) and ethyl acetate (phase O). A solution of 5% w/v of polyvinyl alcohol (PVAL) was obtained in phase W. Then, 400 mg of PLGA were dissolved in 20 mL of phase O and emulsified with 40 mL of PVAL solution by using a homogenizator (ULTRA-TURRAX®; IKA® Works Inc., Wilmington, NC, USA) at 11,000 rpm for 10 min. Afterwards, 160 mL of water without saturation was added to the emulsion in order to allow the diffusion of the organic solvent. After diffusion, the nanoparticles remained in suspension and the solvent was evaporated under reduced pressure at 90 rpm and 30 °C. Nanoparticles were recovered by centrifugation (Optima® LE-80 K; Beckman Coulter Inc., Fullerton, CA, USA) at 25,000 rpm for 20 min, and then washed three times. Finally, they were frozen and lyophilized at 50×10^{-3} mbar and −40 °C for 24 h (FreeZone 6; Labconco®, Kansas City, MO, USA), using mannitol as the cryoprotectant at 1 mg/mL of nanoparticle suspension.

2.2.2. Porous PLGA microspheres

Microspheres were prepared using a modified double emulsion-solvent evaporation method proposed by Kim et al. (2006b). The first emulsion was carried out by stirring with a homogenizator (ULTRA-TURRAX®) at 11,000 rpm for 2 min to mix 8 mL of methylene chloride (in which 500 mg of PLGA were dissolved) and 2.5 mL of a 1% w/v solution of NH_4HCO_3 (porogen agent). Next, this emulsion was poured into 300 mL of a 1% w/v solution of PVAL and stirred at 250 rpm during 4 h using a mechanical stirrer (Caframo™ Limited, Wiarton, Ontario N0H 2T0, Canada). The porous microspheres were recovered by filtration, using a stainless steel mesh with a 10-μm aperture, and dried at room temperature.

2.2.3. Physical characterization

The mean diameter and particle size distribution of the micro- and nano-structures were analyzed using dynamic light scattering (Zetasizer® and Mastersizer®, Malvern Instruments, UK). The morphology of the polymeric nanoparticles and porous biodegradable microspheres was analyzed by Scanning Electron Microscopy (SEM) (JSM-25 S II microscope, JEOL, Japan), and the specific surface area was obtained as indicated in section 2.5.

2.3. Adsorption studies of α-amylase

2.3.1. Adsorption onto porous microspheres

To evaluate protein adsorption behavior, increasing amounts of α-amylase were adsorbed onto porous polymeric microspheres at different pH. First, 25 mg of dried microspheres were immersed into 1 mL of several solutions of the protein. Five concentrations were tested – 2.5, 5.0, 7.5, 10.0 and 12.5 mg/mL – using sodium acetate buffer solution (0.02 M) at pH 4.0 and potassium phosphates buffer solution (0.02 M) at pH 7.2. The samples were labeled as SA, SB, SC, SD and SE, respectively. All samples were gently agitated during 1 h (Water Bath Shaker™, American Optical, USA). The microspheres with adsorbed α-amylase were recovered by filtration and the protein concentration in the supernatant was determined using the bicinchoninic acid assay to ascertain total proteins at 562 nm with a spectrophotometer (Varian Cary 50 Conc, Agilent technologies, Santa Clara, CA, USA). The amount of protein adsorbed (in milligrams) were calculated on the basis of the weight differences between the initial and final concentrations. Three replicates were performed.

2.3.2. Adsorption onto polymeric nanoparticles

Evaluation of the protein adsorption onto polymeric nanoparticles was done by measuring the ζ-potential (zeta-potential) when different amounts of protein were adsorbed. In this step, 100 mg of nanoparticles were re-suspended in 10 mL of sodium acetate buffer at pH 4.0 (0.02 M) during 12 h. Afterwards, 10, 20, 30 and 40 mg of protein were added to the suspensions and subjected to magnetic stirring during 1 h. A nanoparticle suspension with no protein was set as the blank. The ζ-potential of the dispersions was measured using a Zetasizer® (Malvern Instruments, UK) after appropriate dilution with the same buffer solution ($n = 3$).

2.4. Obtaining of the protein drug-delivery system assembled by the adsorption/infiltration process

Briefly, 25 mg of dried porous microspheres were weighed and placed in an eppendorf tube. Simultaneously, a measured amount of polymeric nanoparticles was re-suspended by magnetic stirring (Multistirrer®, Velp Scientifica, USA) in 1 mL of sodium acetate buffer pH 4.0 (0.02 M), during 12 h. The prepared nanoparticle suspensions had 25, 50, 75 and 100 mg/mL. Then, 10 mg of α-amylase were added to each nanoparticle suspension and agitation continued for 1 h more. The suspensions with protein were poured into the eppendorf tube with the porous microspheres and subjected to agitation for 1 additional hour (Water Bath Shaker™, American Optical, USA), in order to infiltrate the nanoparticles with adsorbed protein into the microspheres. The systems were recovered by filtration through a stainless steel mesh (10 μm) and dried at room temperature. These systems were labeled as S2–S5. System S1 was prepared under the same conditions, but without nanoparticle infiltration. The protein content in the remaining suspension was quantified by the bicinchoninic acid assay, and the adsorption efficiency (%AE) was calculated on the basis of the differences between the initial and final concentrations using the following equation:

$$\%\mathrm{AE} = \frac{(C_i - C_f)}{C_i},$$

where, C_i = initial concentration of α-amylase and C_f = concentration of α-amylase in the remaining suspension. Three replicates were done for each nanoparticle concentration ($n = 3$). Finally, to determine the load of nanoparticles in the assembled systems the remaining suspension was frozen and lyophilized at 50×10^{-3} mbar and −40 °C for 24 h (FreeZone 6; Labconco®, Kansas City, MO, USA) to obtain the remaining weight of the nanoparticles after the assembly process. Thus, nanoparticle-loaded efficiency were calculated by the weight differences between the initial amount of nanoparticles and the remaining weight in the final suspension (considering the proportional amount of mannitol per sample).

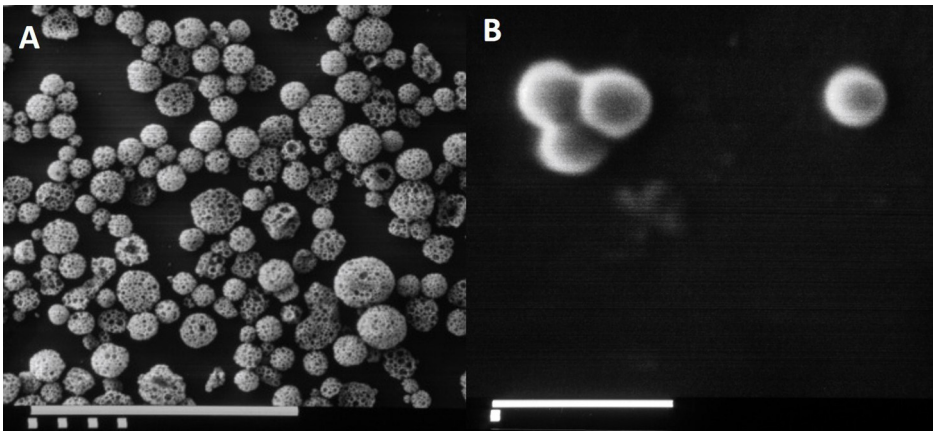

Fig. 1. Scanning electron micrograph of (A) porous polymeric microspheres of PLGA 50:50 (scale bar = 1000 μm) and (B) polymeric nanoparticles of PLGA 50:50 (scale bar = 1 μm).

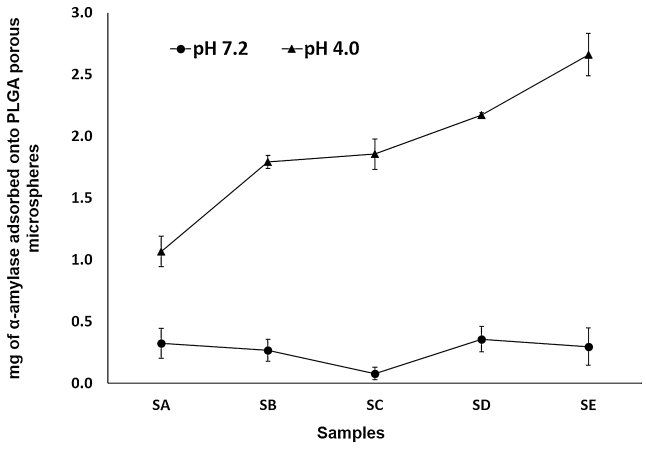

Fig. 2. Amount adsorbed of α-amylase (mg) onto porous microspheres of PLGA at different pH, without nanoparticle infiltration. SA, SB, SC, SD and SE: samples immersed in a solutions with 2.5, 5.0, 7.5, 10.0 and 12.5 mg/mL of protein, respectively.

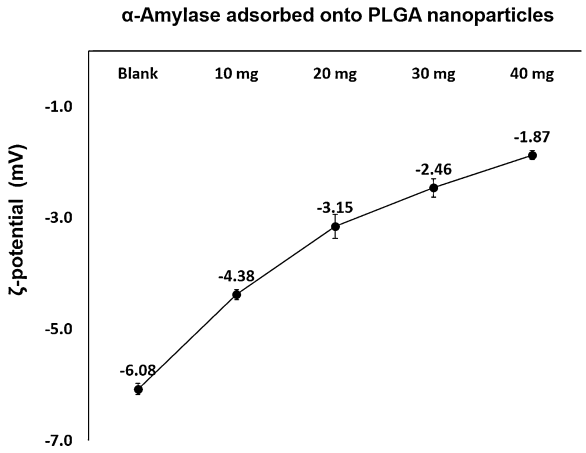

Fig. 3. ζ-potential of NP's adsorbed with increasing amounts of α-amylase at pH 4.0. Blank represents the ζ-potential of the polymeric nanoparticles without protein adsorption. NP's = nanoparticles.

2.5. Measurement of N_2 isotherms

The nitrogen adsorption–desorption isotherms were determined on the free microspheres, polymeric nanoparticles and all the assembled systems (from S1 to S5) using a Bel-Japan Minisorp II apparatus and applying a multipoint technique. Specific surface area was calculated with the Brunauer–Emmet–Teller (BET) equation (Brunauer et al., 1938; Rouquerol et al., 1999) from N_2 adsorption at −196 °C. Because of the low glass transition temperature of the samples, they were out gassed at 30 °C prior to nitrogen adsorption.

2.6. Characterization of the assembled systems by thermal analysis

Differential scanning calorimetry (DSC) and thermogravimetric (TGA) techniques were used to carry out a physical characterization of the assembled systems. For the DSC studies, 2–4 mg of the dried assembled system, pure PLGA and pure α-amylase were placed on aluminum pans and then sealed hermetically. Tests were carried out in a temperature range of 30–280 °C with a 10 °C/min heating rate, under ultrapure nitrogen flux (50 mL/min) (DSCQ10 calorimeter, TA Instruments, USA). Finally, TGA was performed in order to monitor the mass of the system during heating, under the same conditions described above for the DSC studies, but using platinum pans (TGA Q5000IR, TA Instruments, USA).

2.7. In vitro protein release

Potassium phosphate buffer (0.02 M) at pH 7.2 was used as the dissolution medium. The release profiles of all the assembled systems (S1–S5) were obtained. Briefly, 25 mg of each system were weighed on a 5-cm piece of stainless steel mesh (10-μm aperture) and dipped in 10 mL of the dissolution medium before being poured into a glass vial. The vials were transferred to a thermostated bath at 37 °C under magnetic agitation. Afterwards, 100 μL were withdrawn at different times and replaced with fresh medium. "sink conditions" were maintained throughout the study. The amount of α-amylase released at each time was determined by bicinchoninic acid assay ($n = 3$).

2.8. Evaluation of the enzymatic activity of the α-amylase released

The enzymatic activity of α-amylase was evaluated after release from the all the assembled systems. Free α-amylase dissolved in the same conditions was used as a control (buffer pH 7.2 and 37 °C). 2-cChloro-4-nitrophenyl-α-D-maltotrioside (CNP-G3) was the substrate used to measure amylase activity. During the enzymatic reaction, a yellow product was generated: 2-chloro-4-nitrophenol (Foo and Bais, 1998). The assay reagent was prepared using sodium citrate buffer solution (0.01 M) at pH 6.2, CNP-G3 (2.25 mM), sodium chloride (300 mM), calcium chloride (5 mM) and potassium thiocyanate (900 mM). Samples of 75 μL were withdrawn during *in vitro* release studies at 12 h. Samples were placed in assay tubes with 3 mL of the reagent assay previously incubated at 37 °C in a water bath. Once the tubes were agitated by vortex, they were placed back in to the incubation bath. A tube with no sample was set as a blank, then absorbance was measured at 405 nm every minute during 2 min. The α-amylase activity (International Units per liter, U/L) of each sample and control was calculated using the following formula:

$$\alpha\text{–amylase}\left(\frac{U}{L}\right) = \left(\frac{\Delta A}{\min_s} - \frac{\Delta A}{\min_b}\right) \times \frac{\text{TV} \times 1000}{\varepsilon \times \text{SV} \times d},$$

where $\Delta A/\min_s$ = change in the absorbance per minute for the sample or control, $\Delta A/\min_b$ = change in the absorbance per minute for the blank, TV = total volume of the assay (3.075 mL),

Table 1
Characterization of the assembled systems.

System	α-Amylase adsorbed at pH 4.0 (mg)	%AE (%)	NP's Loaded (mg)	Specific surface area $a_{s,\text{BET}}$ (m^2/g)
S1	2.5 ± 0.16	25.2 ± 1.6	0[a]	4.25
S2	2.7 ± 0.29	27.2 ± 2.9	8.1 ± 2.2	2.23
S3	3.8 ± 0.06	37.7 ± 0.6	16.5 ± 1.3	1.94
S4	4.8 ± 0.15	47.4 ± 1.8	32.4 ± 2.4	0.45
S5	5.1 ± 0.12	50.7 ± 1.2	57.9 ± 2.6	–

The results are shown as mean ± standard deviation. S1: system assembled without nanoparticle infiltration; S2–S5: systems with infiltration of nanoparticle suspensions with 25, 50, 75 and 100 mg/mL, respectively. NP's: polymeric nanoparticles; %AE: adsorption efficiency.
[a] System with no nanoparticle infiltration.

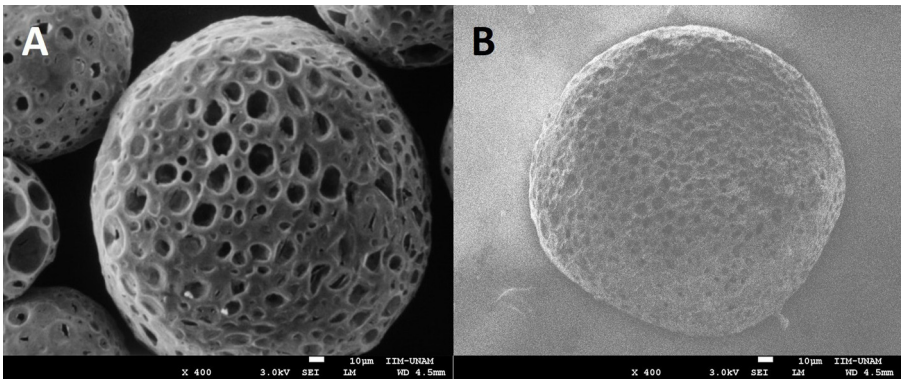

Fig. 4. Scanning electron micrograph of polymeric microspheres of PLGA (50:50). (A) free microspheres and (B) microspheres with infiltrated nanoparticles. (Scale bar = 10 μm).

1000 = conversion from U/mL to U/L, ε = the millimolar extinction coefficient of 2-chloro-4-nitrophenol at 405 nm (12.9), SV = sample volume (0.075 mL) and d = light path (1 cm).

2.9. Evaluation of the conformational structure of α-amylase by circular dichroism spectroscopy (CD)

Each assembled system (from S1 to S5) was placed in 10 mL of phosphate buffer pH 7.2, during 12 h at 37 °C in order to release the α-amylase from the systems. Subsequently, samples of 500 μL were withdrawn and centrifuged at 25,000 rpm for 20 min. The samples were diluted with the same buffer solution until a concentration of 100–400 μg/mL was achieved. CD measurements were performed in a JASCO J-815 spectropolarimeter (Jasco Inc., Easton, MD), equipped with a PFD-425S Peltier-type cell holder for temperature control and magnetic stirring. CD spectra were recorded from 200 to 250 nm, using 1 cm path-length cells. Ellipticities are reported as millidegrees. A CD measurement of free amylase was determined for use as a control.

3. Results

3.1. Obtaining and characterizing system components

The components of the system – the porous microspheres and the polymeric nanoparticles of PLGA – were prepared using the methodology described above. Nanoparticles were solid structures with a main size of 251 ± 2.9 nm, a polydispersity index of 0.08, and a specific surface area of 6.25 m^2/g. The microspheres we obtained were porous structures with a main size of 104 ± 2.7 μm, a uniformity index of 0.61, and a specific surface area of 4.40 m^2/g. The mean diameter of the exposed pores was approximately of 10.2 ± 6.1 μm. The morphologies of solid nanoparticles and porous microspheres are shown in Fig. 1. Kim et al. (2006b) reported how the porosity of microspheres can be controlled using different amounts of ammonium bicarbonate in the first aqueous phase (W_1) during the manufacture of microspheres (Alcalá-Alcalá et al., 2013; Kim et al., 2006b). These characteristics are adequate for carrying out the assembly process based on the adsorption/infiltration of nanoparticles into porous microspheres.

3.2. Studies of adsorption onto micro- and nanoparticles

To select the best pH of the aqueous medium for the adsorption process and the most suitable amount of protein to be added to the systems (protein/microsphere ratio), adsorption studies were performed using two pH values (4.0 and 7.2). Results are presented in Fig. 2. As can be seen, a larger amount of protein adsorbed onto microspheres was achieved at pH 4.0. Based on this finding, we chose pH 4.0 to prepare the assembled systems.

The ζ-potential (zeta-potential) of the free nanoparticles and with increasing amounts of the protein was determined, at pH 4.0, in order to evaluate the influence of the electrostatic forces on the adsorption process, using a electrophoretic light scattering method. Data showed that ζ-potential became more positive as the amount of protein adsorbed increased, see Fig. 3. Changes in ζ-potential could be explained by neutralization of charges during the adsorption process (see Section 4).

3.3. Obtaining and characterizing of the assembled systems

Protein drug-delivery systems assembled by the adsorption and infiltration of polymeric nanoparticles onto porous biodegradable microspheres were prepared using several nanoparticle concentrations. Table 1 show the results for the amount of protein loaded, the adsorption efficiency, and the amount of nanoparticles infiltrated, as well as the specific surface area for all the assembled systems. S1 represents a system without nanoparticle infiltration, but only protein adsorption onto microspheres. It is clear that as the amount of adsorbed nanoparticles increased, the amount of protein in the system also rose. In addition, one can see how the

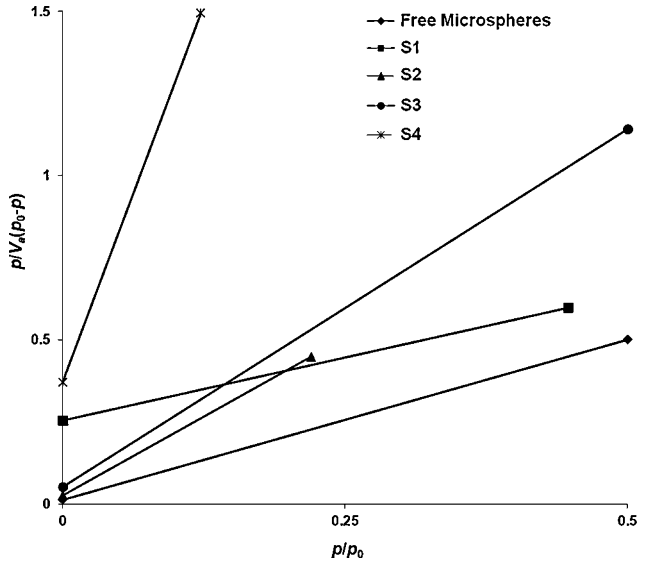

Fig. 5. N_2 isotherms: from top to bottom; (◆) free microspheres of PLGA (50:50); (■) S1: system without nanoparticle infiltration; (▲) S2: system with 25 mg/mL of NP's; (●) S3: system with 50 mg/mL of NP's and (✱) S4: system with 75 mg/mL. NP's = polymeric nanoparticles.

amount of nanoparticles infiltrated increased when a large amount of nanoparticles was in suspension, though this amount seems to reach a maximum, likely related to saturation of the microsphere surface. Fig. 4 shows a porous microsphere saturated with infiltrated nanoparticles compared to a free microsphere.

Fig. 5 presents the N_2 isotherms for all the assembled systems. According to BET theory, the specific surface area is represented by the slope (Brunauer et al., 1938; Rouquerol et al., 1999), such that a steeper slope indicates less surface area. Thus, as can be observed, the slope is higher in S2, S3 and S4 (systems with increasing amounts of infiltrated nanoparticles) compared to S1 (the system with no nanoparticle infiltration) and the free microspheres. The reduction of the surface area shows the loss of surface and saturation as the amount of infiltrated nanoparticles increases.

On the other hand, if the protein is first dissolved and then adsorbed onto both surfaces (micro- and nanoparticles), interaction between the biomolecule and the surfaces takes place at a molecular level. For this reason, thermal studies (DSC and TGA) were performed to understand the interaction of the system's components. DSC thermograms are shown in Fig. 6 and TGA thermograms in Fig. 7 for pure PLGA (50:50), pure α-amylase, and all the assembled systems (from S1 to S5).

The thermal events depicted in the DSC thermograms indicate the presence of a characteristic endothermal peak at 47–52 °C that corresponds to the glass transition temperature (Tg) of the polymeric material (PLGA); however the dehydration event, at ~100 °C, seen in the pure α-amylase thermogram disappeared in all the assembled systems, suggesting that protein is molecularly dispersed on the available surface of the system. Above 200 °C, degradation processes were detected in all DSC thermograms, but were more evident in the assembled systems. Degradation events were followed in TGA thermograms – see Fig. 7 – where it was noted that weight loss was faster in the assembled systems (from S1–S5) than in the pure components.

3.4. In vitro protein release

Protein release studies from the assembled systems were carried out in buffer phosphates, pH 7.2, as the dissolution medium. Release profiles for all systems (S1–S5) are presented in Fig. 8, which shows that in S1 (the system without nanoparticles infiltration) α-amylase was completely released at 24 h. A similar behavior was observed in S2 (system prepared with 25 mg/mL of nanoparticles), but systems S3, S4 and S5 only delivered 73, 45 and 38% of the loaded protein, respectively, at that time. It is suggested that, depending on the degree of saturation, the infiltrated nanoparticles create a physical barrier that reduces the release rate. Different mathematical models have been proposed to explain the mechanism of release from drug-delivery systems (Costa and Sousa-Lobo, 2001), though only the adjustment to the mathematical model proposed by Higuchi was reported because it was the best model that data fit ($r^2 \geq 0.800$). The mathematical model is described as: $M_t/M_\infty = K_H t^{1/2}$; where M_t = the amount of drug released at time t, M_∞ = the total drug has been released, K_H (min^{-1}) = the Higuchi dissolution constant and t = time (Costa and Sousa-Lobo, 2001). Fig. 9 shows the fit of the release profiles to Higuchi's model.

3.5. Enzymatic activity of the released α-amylase and evaluation of its structural integrity

The assembled systems (S1–S5) were placed in a buffer phosphates solution, pH 7.2, at 37 °C, during 12 h in order to release the enzyme. Samples of free α-amylase were treated in the same conditions to be used as a control. Enzymatic activity (UI/L) for all the systems can be observed in Fig. 10, where no significant statistical differences were found in comparison to free α-amylase ($p > 0.05$).

The structural integrity of the released α-amylase was evaluated by circular dichroism. Fig. 11 shows the far-UV CD spectra of α-amylase under the different treatments. Clearly, all the CD spectra are very similar, indicating that there were no appreciable changes in the secondary structure of the amylase when it was released from the assembled systems, as judged by the CD signal.

4. Discussion

4.1. Protein adsorption onto the components of the system (micro- and nanoparticles)

These results show that pH and protein concentration have influence on the adsorption process onto the surface of PLGA

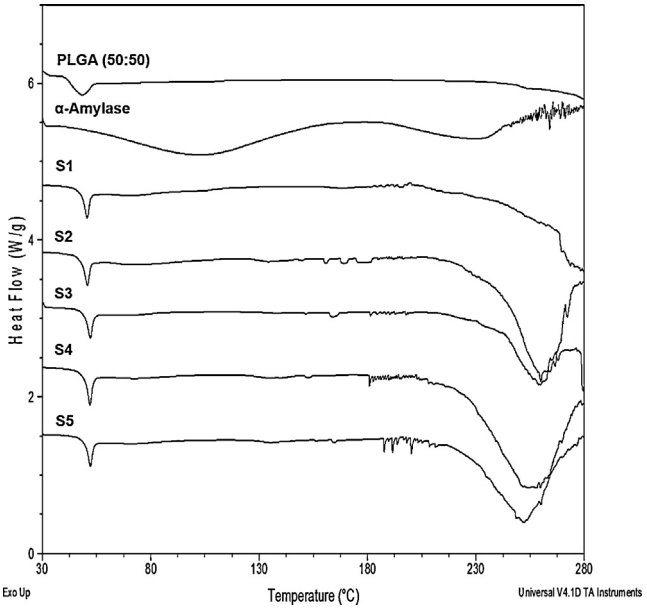

Fig. 6. Differential scanning calorimetric studies. DSC thermograms: from top to bottom; pure PLGA (50:50); pure α-amylase; S1: system assembled without nanoparticle infiltration; S2–S5: systems with infiltration of nanoparticle suspensions with 25, 50, 75 and 100 mg/mL, respectively. NP's = polymeric nanoparticles.

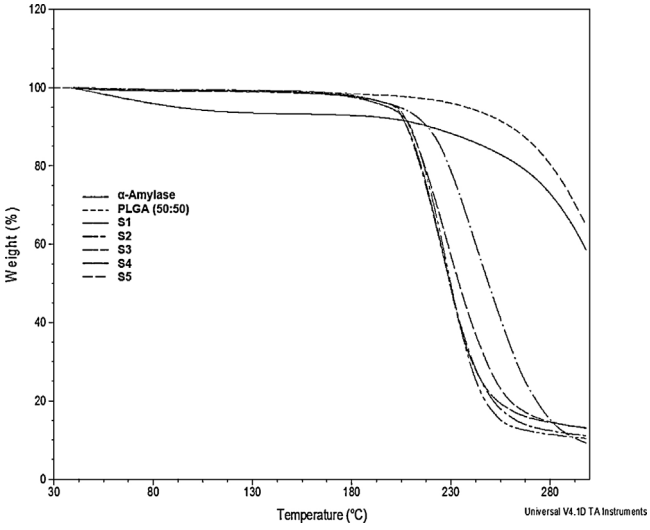

Fig. 7. Thermogravimetric analysis. TGA thermograms: from top to down; α-amylase pure; PLGA (50:50) pure; S1: system assembled without nanoparticle infiltration; S2–S5: systems with infiltration of nanoparticle suspensions with 25, 50, 75 and 100 mg/mL, respectively. NP's = polymeric nanoparticles.

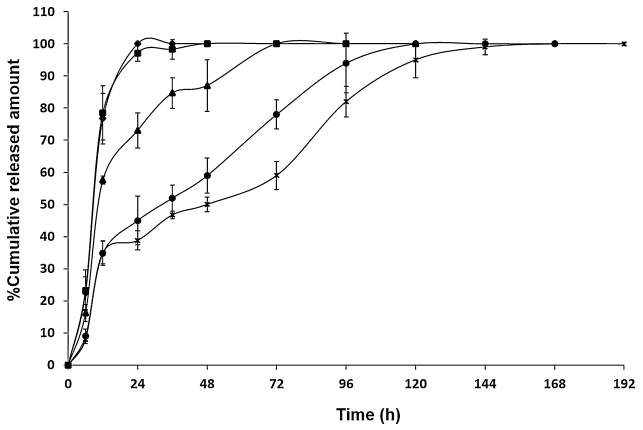

Fig. 8. Release profiles of α-amylase from all assembled systems. Studies performed in phosphates buffer (pH 7.2) at 37 °C. (◆) S1: system without nanoparticles infiltration; (■) S2: system with 25 mg/mL of NP's; (▲) S3: system with 50 mg/mL of NP's; (●) S4: system with 75 mg/mL of NP's and (✱) S5: system with 100 mg/mL of NP's. NP's = polymeric nanoparticles.

microparticles. The isoelectric point of α-amylase is 4.2 (Bautista et al., 1999), while the pK_a of PLGA is 3.8 when the polymer has an end carboxylic group (the polymer used in this work, PLGA 4A, has an acid terminal group). Two pH were tested: a pH of 4.0 where α-amylase is charged positively and the carboxylic groups in PLGA are ionized; and pH 7.2, where both are negatively-charged. More molecules are adsorbed when the medium has an acid pH (4.0) and opposed charges exist. This behavior can be explained by the changes in the properties of the surface of the microspheres and the charges generated in the protein at each pH. Because the process was carried out in an aqueous medium, adsorption is favored. When pH is higher than the isoelectric point, 7.2, the hydrophobic interactions become more important and the adsorption capacity decreases because the microsphere surface presents the same charge as the enzyme. Kondo et al. (1996) and Bautista et al. (1999) described this behavior and the influence of pH when α-amylase is adsorbed onto a hydrophobic surface (Bautista et al., 1999; Kondo et al., 1996), while Li and Li (2007) reported this effect and the role of surface groups when bovine serum albumin is adsorbed onto polymeric PLGA microspheres (Li and Li, 2007). Kim et al. (2006) reported the adsorption of human growth hormone onto porous PLGA microspheres with similar results, though their approach used solvents in order to close the pores (Kim et al., 2006a). Meanwhile, when protein concentration is high, the molecules adsorb close to each other, yielding a higher adsorbed amount that increases when surface area increases and there is less conformational changes (Nakanishi et al., 2001).

The changes observed in ζ-potential confirm the cancellation of charges between the molecules, indicating that electrostatic attractions occur in the aqueous medium at pH 4.0. The charged surface brings the charged proteins nearer to itself and concentrates them there through an attraction phenomenon. Similar effects have been seen when SiRNA is adsorbed onto chitosan-coated-PIBCA nanoparticles (Martimprey et al., 2010). Therefore, electrostatic interactions must be considered to obtain better adsorption efficiencies and increase the amount of drug on the surface. Low adsorption efficiencies have been reported when organic solvents and other structures, like silicon microparticles, are used to adsorb peptides, since no electrical attractions occur (Kilpeläinen et al., 2011).

4.2. Systems assembled by adsorption/infiltration

With the use of the adsorption/infiltration method, assembled systems can be prepared at different levels of saturation that show a clear interdependence between the amount of nanoparticles infiltrated and the amount of protein adsorbed. This finding is related to the fact that protein is adsorbed on both surfaces (micro- and nano-particles) since the structures or components of the system are immersed in the same solution in which the protein is dissolved. In addition, there is more available surface area when the amount of nanoparticles in suspension is greater. Because the

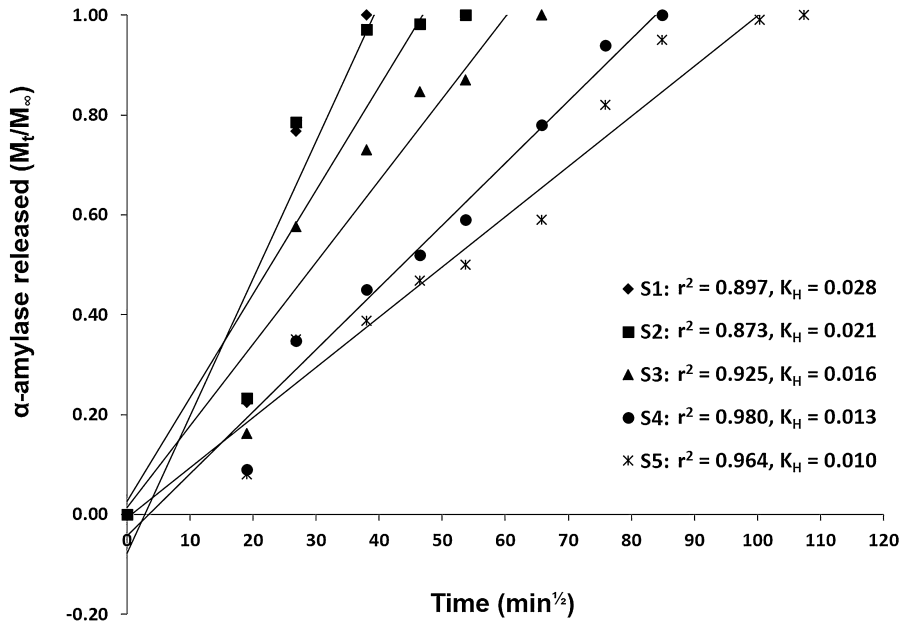

Fig. 9. Fit of the release profiles of α-amylase to the Higuchi's model. (◆) S1: system without nanoparticles infiltration; (■) S2: system with 25 mg/mL of NP's; (▲) S3: system with 50 mg/mL of NP's; (●) S4: system with 75 mg/mL of NP's and (✱) S5: system with 100 mg/mL of NP's. NP's = polymeric nanoparticles. M_t/M_∞ = amount released at time t/amount total released. K_H (min^{-1}) = Higuchi dissolution constant. r^2 = coefficient of determination.

amount of microspheres was constant during the assembly, the surface area offered by the nanoparticles is the main factor involved in obtaining better adsorption efficiencies because the area increases when the concentration of nanoparticles increases. Similar results were achieved in a previous study, where a peptide – leuprolide acetate, a small nonapeptide – was used as a drug model (Alcalá-Alcalá et al., 2013). The saturation process is explained by the reduction of the specific surface area in the assembled systems, see Fig. 5. Fig. 5 also shows how the surface area of the system S1 (with no infiltration of nanoparticles) and the free microspheres are not so different; thus it is suggested that the reduction of the surface area is mainly due to the adsorption and formation of a nanoparticle film on the surface of the porous microsphere.

Thermal analysis showed the molecular interaction of the protein with the polymer in the assembled systems because the characteristic peaks of protein thermograms are not present in the system thermograms. This can be related to a molecular dispersion of the protein over the entire porous polymeric matrix. However, small movements in the Tg of PLGA in the system thermograms can be detected in comparison to pure PLGA. This finding could be associated with rearrangements and interfacial segregation of the polymer after the manufacturing processes involving micro- and nano-structures (Bouissou et al., 2006). TGA studies evidence how the loss of weight in the assembled systems begins at approximately at 190 °C and is more pronounced than in the pure components, indicating that molecular interactions occur between the protein and PLGA during the adsorption/infiltration assembly process.

4.3. Protein release

The dominant mechanism of protein release from the assembled system is passive diffusion associated with a concentration gradient. The porous structure allowed water to penetrate into the polymeric matrix from the dissolution medium, thus dissolving the adsorbed protein and returning it to the medium. The profiles shown in Fig. 8 fit Higuchi's model, indicating a release mechanism associated with Fickian diffusion, which could be related to the water passing through the pore channels (see Fig. 9). Mao et al. (2007) described the influence of surface porosity and the internal morphology of PLGA microspheres on the release behavior of hydrophilic molecules, and reported that the initial release phase is mainly characterized by pore diffusion (Mao et al., 2007). The "burst effect" observed in all release profiles could be related to the protein adsorbed onto more external surfaces. Sun et al. (2009) and Kilpeläinen et al. (2011) found the same effect when human serum albumin (protein model) and melotan II (peptide model) were adsorbed onto polymeric and silicone surfaces, respectively (Kilpeläinen et al., 2011; Sun et al., 2009). Finally, Fig. 8 clearly shows how the release rate is modified after 24 h; thus, the increasing amount of nanoparticles inside the porous microspheres causes a decline in the release rate. The infiltrated nanoparticles tend to form a film on the microsphere surface that becomes more continuous when the amount of nanoparticles inside the microsphere is large, and so acts as a physical barrier that modifies the release rate (Alcalá-Alcalá et al., 2013).

As observed in Fig. 9, coefficients of determination (r^2) indicate that more than 80% and up to 98% of the data variation of the release profiles can be explained with the Higuchi's model. The coefficients of determination increased from the system S1–S5; thus, there is a better fit to the model when systems are more saturated with adsorbed nanoparticles, so that the systems behave as a matrix-type system. This model is used to describe the drug dissolution from several types of modified release pharmaceutical dosage forms like matrix-type systems loaded with water soluble drugs (Costa and Sousa-Lobo, 2001). An important event that can be seen is the decreasing in the Higuchi dissolution constant (K_H) from the system S1–S5, which explains how the release rate decreased as the porous microspheres were more saturated with nanoparticles.

4.4. Protein integrity studies

An assay of α-amylase is used to diagnose of acute pancreatitis. There are several methods for measuring of the activity of this enzyme that employ some nitrophenylated oligosaccharides as the substrate, which releases a chromophore such as 4-nitrophenol. One example is the substrate 2-chloro-4-nitrophenyl maltotriose (CNP-G3), which is hydrolyzed by α-amylase in the presence of high thiocyanate concentrations with no lag phase. The enzymatic reaction produces a yellow compound (2-chloro-4nitrophenyl) that can be monitored spectrophotometrically at 405 nm. This method is sensitive, precise and free of interferences (Foo and Bais, 1998). No significant differences were found between free α-amylase and the enzyme that was released from the assembled systems. Studies have described that the affinity of α-amylase for solid surfaces at high pH (release at 7.2 and activity assay at 6.2) reduces the extent of conformational changes and increases its relative activity (Kondo et al., 1996). Meanwhile certain enzymes acquire their native form in a reversible way after the desorption process when they come into contact with their substrates. Indeed,

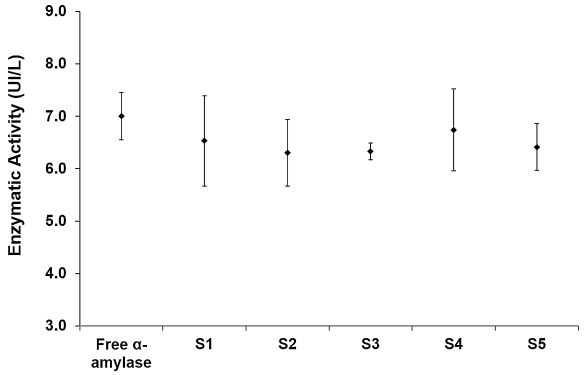

Fig. 10. Enzymatic activity of α-amylase. Assays were performed in citrates buffer (pH 6.2), at 37 °C, using CNP-G3 as substrate. S1: system assembled without nanoparticle infiltration; S2–S5: systems with infiltration of nanoparticle suspensions with 25, 50, 75 and 100 mg/mL, respectively. NP's = polymeric nanoparticles.

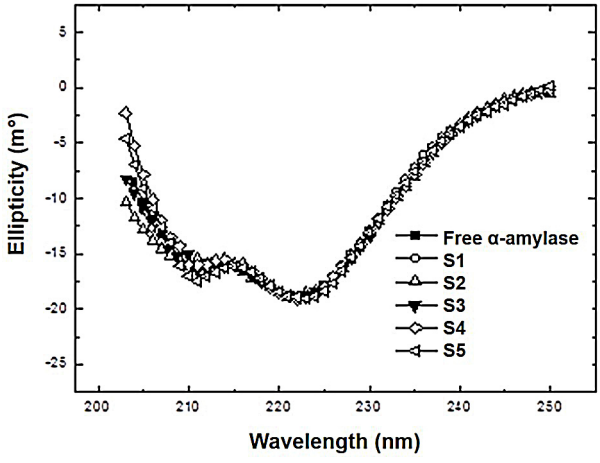

Fig. 11. Far-UV CD spectra of α-amylase after different treatments. Spectra were recorded in 20 mM of phosphates buffer (pH 7.2), at 37 °C. S1: system assembled without nanoparticle infiltration; S2–S5: systems with infiltration of nanoparticle suspensions with 25, 50, 75 and 100 mg/mL, respectively. NP's = polymeric nanoparticles.

a reversible process can be seen in which proteins were adsorbed onto a surface with an opposite electric charge and at high concentrations, favoring surface crystallization with a more densely-packed arrangement (Nakanishi et al., 2001).

The CD spectra obtained for α-amylase are similar to those reported by Matsuo et al. (2005), who studied the secondary structure of several proteins, including this enzyme (Matsuo et al., 2005). As there were no changes in the secondary structure of α-amylase or in its conformation, it can be inferred that its activity was not be affected. These findings show that the assembly process by adsorption/infiltration is a useful tool for formulating sensitive drugs, like proteins, because no damage in their secondary structure is found after they are adsorbed and then released.

5. Conclusions

An adsorption/infiltration process was used to obtain an injectable protein drug-delivery system using α-amylase as the protein model. This method makes it possible to load proteins in an environment that is friendly to this kind of molecules because the common physicochemical stress of a process like microencapsulation is avoided during formulation. Therapeutic doses can be loaded because the protein is adsorbed first onto nanoparticles and then onto the microsphere surface. Additionally, the nanoparticles inside the microsphere saturate the surface of the system at different levels. The degree of saturation modifies the release velocity as amount of nanoparticles increases. Therefore, depending on required dose frequency, a specific system can be prepared. The properties of the α-amylase, such as its primary structure and isoelectric point, the properties of the polymers and surfaces, the pH of the aqueous medium, and the protein concentration, all play an important roles in adsorption efficiency, so the influence of these factors on the integrity of the molecule during formulation must be considered. In order to evaluate the efficacy of this novel drug-delivery system the enzymatic activity of α-amylase was determined for all assembled systems, but no significant changes were found in comparison to a sample of the free enzyme. Finally, conformational studies by circular dichroism basically showed no significant changes in the secondary structure once the protein was adsorbed and then released. This study emphasizes on the potential use of this approach to formulate sensitive drugs like biomolecules as a feasible alternative that resolves the inconveniences of preparing protein drug-delivery systems using conventional processes that compromise molecule stability at every step of the manufacturing process.

Conflict of interest

The authors affirm that they have no conflicts of interest regarding this work.

Acknowledgements

Financial support from DGAPA (project PAPIIT IN222411, PAPIIT 2019143 and CONACYT CB-221629) is gratefully acknowledged. Sergio Alcalá thanks to CONACYT for the student grant (223443) and to UNAM for doctoral studies. The authors thank to QFB Damaris Cabrero for her assistance in TGA testing.

References

Alcalá-Alcalá, S., Urbán-Morlán, Z., Aguilar-Rosas, I., Quintanar-Guerrero, D., 2013. A biodegradable polymeric system for peptide–protein delivery assembled with porous microspheres and nanoparticles, using an adsorption/infiltration process. Int. J. Nanomed. 8, 2141–2151.
Bautista, L.F., Martınez, M., Aracil, J., 1999. Adsorption equilibrium of α-amylase in aqueous solutions. AIChE J. 45 (4), 761–768.
Bouissou, C., Rouse, J.J., Price, R., van der Walle, C.F., 2006. The influence of surfactant on PLGA microsphere glass transition and water sorption: remodeling the surface morphology to attenuate the burst release. Pharm. Res. 23 (6), 1295–1305.
Brunauer, S., Emmett, P.H., Teller, E., 1938. Adsorption of gases in multimolecular layers. J. Am. Chem. Soc. 60, 309–319.
Costa, P., Sousa-Lobo, J.M., 2001. Modeling and comparison of dissolution profiles. Eur. J. Pharm. Sci. 13, 123–133.
Dai, C., Wang, B., Zhao, H., 2005. Microencapsulation peptide and protein drugs delivery system. Colloids Surf. B: Biointerfaces 41, 117–120.
Degim, I.T., Çelebi, N., 2007. Controlled delivery of peptides and proteins. Curr. Pharm. Des. 13, 99–117.
Foo, A.Y., Bais, R., 1998. Amylase measurement with 2-chloro-4-nitrophenyl maltotrioside as substrate. Clin. Chim. Acta 272, 137–140.
Frokjaer, S., Otzen, D.E., 2005. Protein drug stability: a formulation challenge. Nat. Rev. 4, 298–306.
Fu, K., Klibanov, A.M., Langer, R., 2000. Protein stability in controlled-release systems. Nat. Biotechnol. 18, 24–25.
Kilpeläinen, M., Mönkäre, J., Vlasova, M.A., 2011. Nanostructured porous silicon microparticles enable sustained peptide (Melanotan II) delivery. Eur. J. Pharm. Biopharm. 77, 20–25.
Kim, H.K., Chung, H.J., Park, T.G., 2006a. Biodegradable polymeric microspheres with open/close pores for sustained release of human growth hormone. J. Control. Release 112 (2), 167–174.
Kim, T.K., Yoon, J.J., Lee, D.S., Park, T.G., 2006b. Gas foamed open porous biodegradable polymeric microspheres. Biomaterials 27, 152–159.
Kondo, A., Urabe, T., Yoshinaga, K., 1996. Adsorption activity and conformation of a-amylase on various ultrafine silica particles modified with polymer silane coupling agents. Colloids. Surf. A 109, 129–136.
Krishnamurthy, R., Manning, M.C., 2002. The stability factor: importance in formulation development. Curr. Pharm. Biotechnol. 3 (4), 361–371.
Li, W., Li, S., 2007. A study on the adsorption of bovine serum albumin onto electrostatic microspheres: role of surface groups. Colloids Surf. A 295, 159–164.
Manning, M.C., Chou, D.K., Murphy, B.M., Payne, R.W., Katayama, D.S., 2010. Stability of protein pharmaceuticals: an update. Pharm. Res. 27 (4), 544–575.
Mao, S., Xu, J., Cai, C., 2007. Effect of WOW process parameters on morphology and burst release of FITC-dextran loaded PLGA microspheres. Int. J. Pharm. 334, 137–148.
Martimprey, H., Bertrand, J.R., Malvy, C., Couvreur, P., Vauthier, C., 2010. New core–shell nanoparticles for the intravenous delivery of siRNA to experimental thyroid papillary carcinoma. Pharm. Res. 27 (3), 498–509.
Matsuo, K., Yonehara, R., Gekko, K., 2005. Improved estimation of the secondary structures of proteins by vacuum-ultraviolet circular dichroism spectroscopy. J. Biochem. 138, 79–88.
Nakanishi, K., Sakiyama, T., Imamura, K., 2001. On the adsorption of proteins on solid surfaces, a common but very complicated phenomenon. J. Biosci. Bioeng. 91 (3), 233–244.
Pavlou, A.K., Reichert, J.M., 2010. Recombinant protein therapeutics-success rates, market trends and values to 2010. Nat. Biotechnol. 22 (12), 1513–1519.
Putney, S.D., 1998. Encapsulation of proteins for improved delivery. Curr. Opin. Chem. Biol. 2 (4), 548–552.
Quintanar-Guerrero, D., Fessi, H., Allémann, E., Doelker, E., 1996. Influence of stabilizing agents and preparative variables on the formation of poly(D,L-lactic acid) nanoparticles by an emulsification–diffusion technique. Int. J. Pharm. 143, 133–141.
Rodríguez-Cruz, I.M., Domínguez-Delgado, C.L., Escobar-Chávez, J.J., 2009. Nanoparticle infiltration to prepare solvent-free controlled drug delivery systems. Int. J. Pharm. 371, 177–181.
Rouquerol, J., Rouquerol, F., Sing, K., 1999. Adsorption by Powders and Porous Solids. Academic Press, San Diego, USA.
Shah, R.B., Schwendeman, S.P., 2014. A biomimetic approach to active self-microencapsulation of proteins in PLGA. J. Control. Release 196, 60–70.
Spada, G., Gavini, E., Giunchedi, P., 2011. Protein delivery from polymeric nanoparticles. World Acad. Sci. Eng. Technol. 52, 245–249.
Sun, L., Zhou, S., Wang, W., 2009. Preparation and characterization of porous biodegradable microspheres used for controlled protein delivery. Colloids Surf. A 345, 173–181.
Tan, M.L., Choong, P.F.M., Dass, C.R., 2010. Recent developments in liposomes: microparticles and nanoparticles for protein and peptide drug delivery. Peptides 31, 184–193.
Van der Weert, M., Hennink, W.E., Jiskoot, W., 2000. Protein instability in poly (lactic-*co*-glycolic acid) microparticles. Pharm. Res. 17, 1159–1167.
Vrignaud, S., Benoit, J.P., Saulnier, P., 2011. Strategies for the nanoencapsulation of hydrophilic molecules in polymer-based nanoparticles. Biomaterials 32, 8593–8604.
Wang, W., 1999. Instability, stabilization, and formulation of liquid protein pharmaceuticals. Int. J. Pharm. 185, 129–188.